Summer 2018

Fluid flow in a Krogh cylinder: A model for a single capillary and surrounding tissue

Xianjie Qiu

FLUID FLOW IN A KROGH CYLINDER: A MODEL FOR A SINGLE CAPILLARY AND SURROUNDING TISSUE

by

XIANJIE QIU

A THESIS

Presented to the Faculty of the Graduate School of the

MISSOURI UNIVERSITY OF SCIENCE AND TECHNOLOGY

In Partial Fulfillment of the Requirements for the Degree

MASTER OF SCIENCE IN MECHANICAL ENGINEERING

2018

Approved by

DR. Parthasakha Neogi, Advisor
Dr. Dipak Barua
Dr. Joontaek Park

ABSTRACT

A model describing the flow of plasma from the capillaries to the interstitial space in the extravascular tissue and back into the capillaries is constructed and solved. The flow through the tissue or the interstitial spaces is described by the Brinkman equation for porous medium, modified to account for the presence of cells considered as spheres. The flow of blood through the capillaries is considered to be that of a Newtonian fluid. The flow between capillary and tissue is coupled by the permeability of the capillary wall. The nature of flow and its magnitude was found to be highly dependent on the values of the coupling constants which relate the resistances to plasma flow in the extravascular space and the capillary. The flow in the extravascular tissue is found to be very low. The flow profiles show that there is mixing of the interstitial fluid in the extravascular tissue. It is shown here that local flow of plasma both in the extravascular space and lymph flow. This model bridges the gap between Krogh cylinders when only diffusion is considered, and stirred tanks where convection is dominant. The model also consider the leaky effect, and compare the health liver and tumor tissue.

ACKNOWLEDGMENTS

First and foremost, I want to thank my advisor, Dr. Parthasakha Neogi for his invaluable guidance and help through so many challenges during my graduate studies at Missouri University of Science and Technology. Along with him, my committee members, Dr. Dipak Barua and Dr. Joontaek Park, also helped me by providing helpful tips and comments and encouraging me constantly. I am very grateful. Drs. Neogi and Park provided excellent teaching for transport phenomena, which emphasized the significance of this research work and helped understand basic facts and concepts. Dr. Chen Hou also provided help and taught me the knowledge of human physiology. I am grateful to my parents, Mr. Zuguo Qiu and Mrs. Xiaolan Luo, for all their support and encouragement they provided to me to pursue my graduate work.

Finally, I would like to thank the department chair, Dr. Muthanna H. Al-Dahhan, and secretaries, Ms. Marlene Albrecht, Ms. Emily Kost, and Ms. Dawn Schacht for taking care of all the administrative work for me during my graduate studies.

Again, I am very grateful to have Dr. Neogi during my graduate studies and definitely believe he can help me grow a stronger presence in my academic career.

TABLE OF CONTENTS

LIST OF ILLUSTRATIONS

LIST OF TABLES

NOMENCLATURE

Symbol	Description
$\Delta\wp$	Pressure difference
σ	Reflection coefficient
Π	Osmotic pressure difference
U	Urinary excretion
Q_i	Quantity plasma input
C_{pl}	Plasma in the capillary
L_i	Flow to the lymphatic system
R	Radius of total tissue
r_o	Outer radius of the capillary
r_i	Inner radius of the capillary
Z	Total Length of capillary and tissue
L	Length of the capillary
k	Porous medium of permeability
L_p	Membrane hydraulic coefficient
μ	Viscosity of plasma
K	Conductivity
ω	Fraction fluid lost
Δp	Pressure drop
v_r	Radial velocity in the extravascular space
v_z	Axial velocity in the extravascular space
s	As defined as in Eq. (3.10)

ξ	Non-dimensional r, sr
ζ	Non-dimensional z, sz
P	As defined as in Eq. (3.13)
X	As defined as in Eq. (3.14)
Q	As defined as in Eq. (3.16)
U_0	As defined as in Eq. (3.17)
U_1	As defined as in Eq. (3.19)
c_i	Constants of integration for solution in the extravascular space
α_i	Constants of integration for solution in the extravascular space
ψ	Stream function of flow through the extravascular space
$\wp$	Pressure in the interstitial
$\hat{c}_i$	Constants of integration for solution in the capillary
$\hat{\alpha}_i$	Constants of integration for solution in the capillary
$\hat{\psi}$	Stream function of flow through the capillary
$\hat{v}_z$	Axial velocity in the capillary
$\hat{v}_r$	Radial velocity in the capillary
$\hat{\wp}$	Pressure in the capillary
Λ	Non-dimensional L, sL
ξ_i	Non-dimensional r_i, sr_i
ξ_0	Non-dimensional r_o, sr_o
α	Ratio of resistance to flow in porous medium to resistance of flow through the capillary wall, as defined as in Eq. (3.40)
β	Ratio of resistance to flow through the capillary to resistance of flow through the capillary wall, as defined as in Eq. (3.41)

γ	As defined as in Eq. (3.42)
a_n	Constant of separation
μ_r	As defined as in Eq. (3.44)

1. INTRODUCTION

1.1. SIGNIFICANCE OF THE STUDY

Death rate from cancer is very high. The traditional treatment of tumors generally involves two steps – surgical removal of tumor or radiation therapy and chemotherapy subsequent therapeutic management of residual cancer cells. Chemotherapy, also called "chemo", is the use of strong drugs to kill cancer cells. Drugs are chosen which depend on the kind of cancer and how much cancer is in human body. However, the drug treatments are not able to remove all of malignant tumors in most cases of clinical application, although the drug could stop their growth. The delivery of chemo into cancer tissue is also a problem, as the drug relies on permeability and retention. Chemotherapy causes different levels of damage to normal tissue cell when the drug acts to destroy growing cancer cells. One of the explanations is related to the microvascular network is heterogeneity and the cancer cell will destroy and increase permeability of the microvascular tissue. The leaking blood vessel will decrease the lymphatic function and raise interstitial pressure (Guyton and Hall, 2000, pp185). Hence, in order to devise the dosage strategies to the patient, the models that predict the bloodstream transfer from capillary to tissue become important.

1.2. BACKGROUND INFORMATION

In order to simulate the flow of plasma from the capillary vessel to extravascular tissue, we begin with the description of basic circulation below and then on to flow at lower scales.

- The Circulatory System

The blood vessels form a closed circuit to and from the heart. The human vessel system has two circuits: pulmonary circuit and systemic circuit (Figure 1.1). Pulmonary circuit sends the blood to the lungs for oxygenation. This process begins from the right ventricle, which receives the deoxygenated blood from right atrium, and pumps the oxygen lean blood to pulmonary right and left arteries to unload the carbon dioxide and receive the oxygen. Systemic circuit supplies oxygen and nutrients via blood from left ventrium to brain and all body, and then disposes the waste.

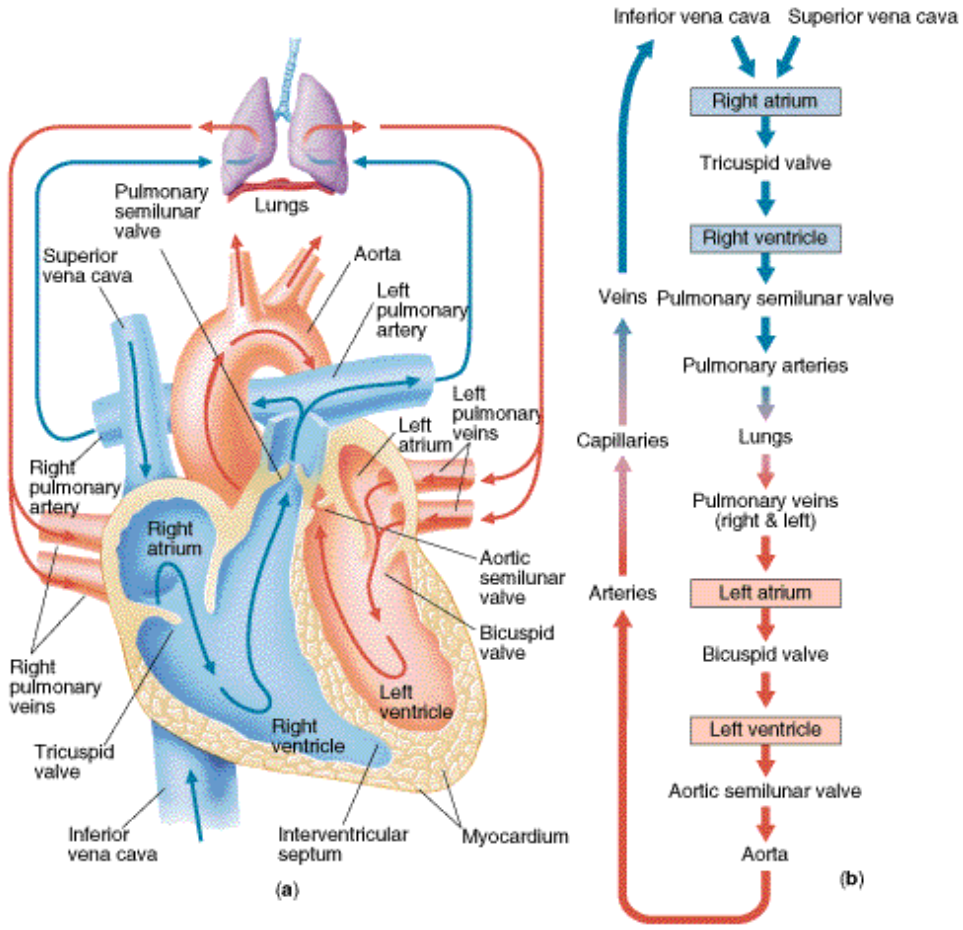

Figure 1.1 Schematic view of the main circulation.

The blood vessels are organs of the cardiovascular system and there are different types of blood vessels (Figure 1.2) having different functions. They include:

Arteries - carry blood away from the heart at high pressure, with thick strong elastic walls (three layers or tunics): endothelial lining, middle layer of smooth muscle and elastic tissue and outer layer of connective tissue.

Arterioles - receive blood from the arteries and carry blood to the capillaries. It has thinner wall than an artery (three layers or tunics): endothelial lining, middle and outer layers are thinned. Arterioles has some smooth muscle tissue and small amount of connective tissue, helps control blood flow into a capillary

Capillaries - sites of exchange of substances between the blood and the body cells. They are the smallest diameter blood vessels, connect the smallest arteriole and the smallest venule. Capillaries are extensions of the inner lining of arterioles and the walls are endothelium only and semi-permeable.

Venules - receive blood from the capillaries. Microscopic vessels continue from the capillaries and merge to form veins, with walls thinner than arterioles, less smooth muscle and elastic tissue than arteriole.

Veins - carry blood toward the atria of the heart, thinner walls than arteries (three layers or tunics) and under relatively low pressure. Middle wall is poorly developed, and many have flap-like valves. Thus, there is one other functions which is that of blood reservoir. It ensures a normal blood flow even when as much as 25% of blood is lost.

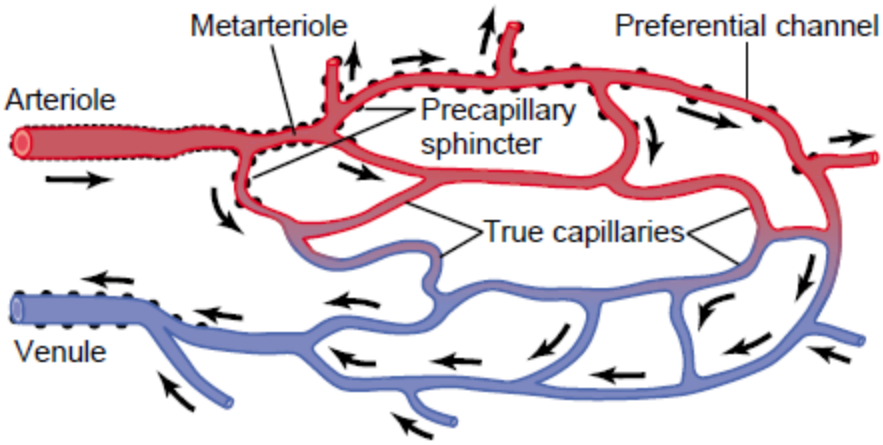

Figure 1.2 Schematic view of the mesenteric capillary bed (Redrawn from Zweifach (1950), reproduced from Guyton and Hall 2000.).

1.3. MICROCIRCULATION, CAPILLARY WALL, AND THE INTERSTITUM

Microcirculation refers to the blood circulation between the arterioles and the venules. Microcirculation is not only a pathway for circulation, but also a place for material exchange. The capillary wall (Figure 1.3) consists of a single layer of endothelial cells with a basal lamina membrane on the outside. The total thickness of membrane is about 0.15-0.50 μm and the split between the endothelial cells at intervals of about 10-20 nm. The water in the plasma and in the tissue fluid, various nutrient substances, and small-molecule organic substances can easy pass through the form of diffusion or filtration-reabsorption. The lipid bilayer of the endothelial cell membrane is the direct pathway for the diffusion of O_2, CO_2 and fat-soluble substances. In addition, the transport of macromolecules can also be achieved by the active transport of capillary endothelial cells.

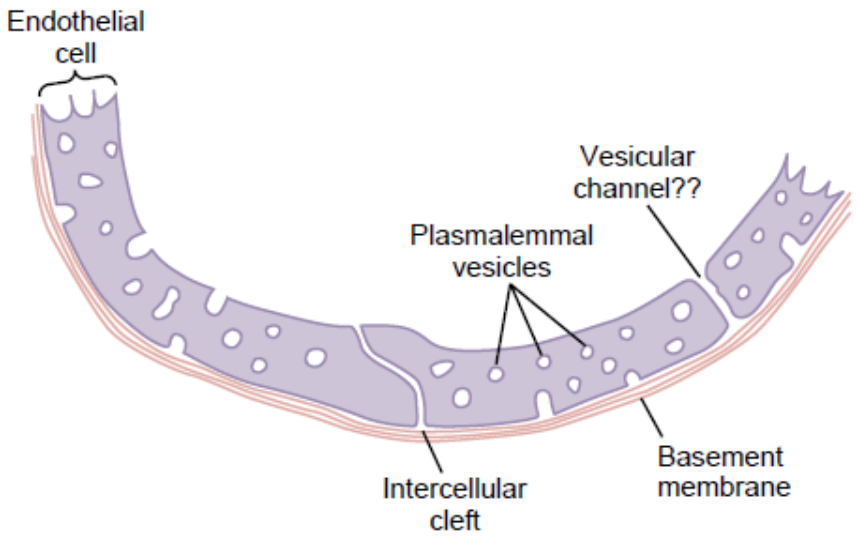

Figure 1.3 Schematic view of capillary wall. From Guyton and Hall (2000).

In animals, tissue fluid penetrates from the end of the capillary artery into a portion of the fluid in the interstitial space. After exchanging substances with the tissue cells, it returns to the blood or lymph through the capillary vein end or lymphatic capillaries. The structure as shown below Figure 1.4.

Most of the tissue fluids are in a gel state and cannot flow. Therefore, they will not flow down to the lower part of the body due to gravity. Inserting the injection needle into the interstitial space will not allow the tissue fluid to be withdrawn. However, the water in the gel and the diffusive movements dissolved in water and various solute molecules are not hindered by the gel and can still exchange substances with blood and intracellular fluids. Tissue fluid is produced by the filtration of blood plasma at the arterial end of the capillary, and at the end of the capillary vein, most of is absorbed back by the blood and through the wall of the capillary.

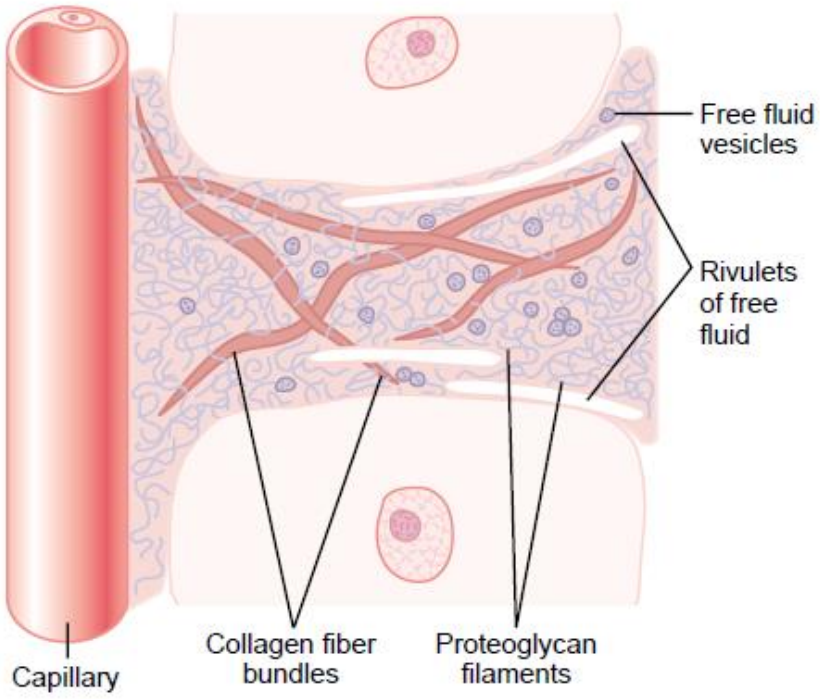

Figure 1.4 Schematic view of the endothelium. From Guyton and Hall (2000).

1.4. PRIMARY CONDITIONS RELATE TO FLUID MOVEMENT THROUGH THE CAPILLARY MEMBRANE AND VARIATION

As previously mentioned, the capillaries connect the arteriole and the venule, and they are semi-permeable. The system of blood fluid across capillary membrane to tissue exchange is determined by diffusion, hydrostatic and osmotic pressure, and also other capillary filtration coefficients, (Jain, 1998)

1.4.1. Fundamental of Forces Fluid Movement. Described below are the four pressures that control the fluid exchange between capillary and interstitial space,

- Capillary pressure, which drives the blood flow outward from inside capillary to outside tissue. The blood pressure move the blood through the

arteries and arterioles. At the ends, arteriole has higher pressure than venule. This flow and diffusion are the agencies for moving water, oxygen, and nutrients, around.

- Interstitial fluid pressure, which drives fluid inward back to capillary through membrane. The interstitial space also contains the fluid, but its pressure is augmented by osmotic pressure, so that the main direction of the fluid is inward to tissue.
- Plasma colloid osmotic pressure, which takes the blood fluid back to vessel through the membrane. The blood contain the plasma proteins, which cannot leak into tissue due to the semi-permeable. Plasma proteins use to maintain the hydrostatic pressure which favors to reabsorb.
- Interstitial fluid colloid osmotic pressure, which is inclined osmosis of fluid outward through the capillary membrane and oppose to hydrostatic pressure. It is formed by tissue protein and use to pull out the fluid from capillaries.

The driving force leads the pressure difference $\Delta\wp$, and the osmotic pressure $-\sigma\Delta\Pi$, where σ is the reflection coefficient. These forces combine and provide the driving force for blood flow in the capillary and tissue net at any location and become $\Delta\wp - \sigma\Delta\Pi$. Here Π is the osmotic pressure difference.

1.4.2. Variation of the Force Along Capillary Length. Four driving forces push the plasma along the capillary, then outward and inward. At the beginning of the capillary, the total outward force is 13mm Hg, which moves the fluid to the extravascular tissue. At the end of capillary, the total force drives the fluid back into capillary, and the

total inward force is 7 mm Hg. During the transportation, the excess fluid in extravascular tissue enters the lymphatic system. The Table 1.1 and Table *1.2* present details data between the plasma fluid and the interstitial fluid from Guyton and Hall (2000).

Table 1.1 Forces Tending to Move Fluid Outward at the Arterial End.

Forces tending to move fluid inward	mm Hg
Capillary pressure at the atrial end	30
Negative pressure free fluid pressure	3
Interstitial fluid colloid osmotic pressure	8
Total outward force	41
Forces tending to move fluid inward	
Plasma colloid osmotic pressure	28
Total inward force	28
NET OUTWARD FORCE	13

Table 1.2 Forces Tending to Move Fluid Inward at the Venous End.

Forces tending to move fluid inward	mm Hg
Capillary pressure at the atrial end	10
Negative pressure free fluid pressure	3
Interstitial fluid colloid osmotic pressure	8
Total outward force	21
Forces tending to move fluid inward	
Plasma colloid osmotic pressure	28
Total inward force	28
NET INWARD FORCE	7

1.4.3. Starling Equilibrium. Starling equilibrium illustrates the average pressures in the capillary. The force data change as the capillary location, and the state of near-equilibrium exists at the capillary membrane. The amount of fluid filtered out of the capillaries at the end of the artery is almost exactly equal to the amount of fluid reabsorbed at the venous end. There is a slight imbalance, which explains the return of the lymphatic system to the circulating fluid. Table 1.3 present the principle of Starling convective equilibrium. The table shows the mean capillary pressure at the two ends. It gives the average functional pressure over the entire length of the capillary. For the total capillary circulation, the total average external force is 28.3 mm Hg and the total average internal force is 28 mm Hg. A slight imbalance of 0.3 mmHg causes slightly more inflow into the interstitial space than in the inflow capillary due to a net filtration of plasma, which fluid enter to the lymphatic circulation.

Table 1.3 Mean Forces Tending to Move Fluid across the Capillary Membrane.

Forces tending to move fluid inward	mm Hg
Capillary pressure at the atrial end	17.3
Negative pressure free fluid pressure	3
Interstitial fluid colloid osmotic pressure	8
Total outward force	28.3
Forces tending to move fluid inward	
Plasma colloid osmotic pressure	28
Total inward force	28
NET INWARD FORCE	0.3

Pressures are important in modeling the flow conditions. By using above table we can provide an overview.

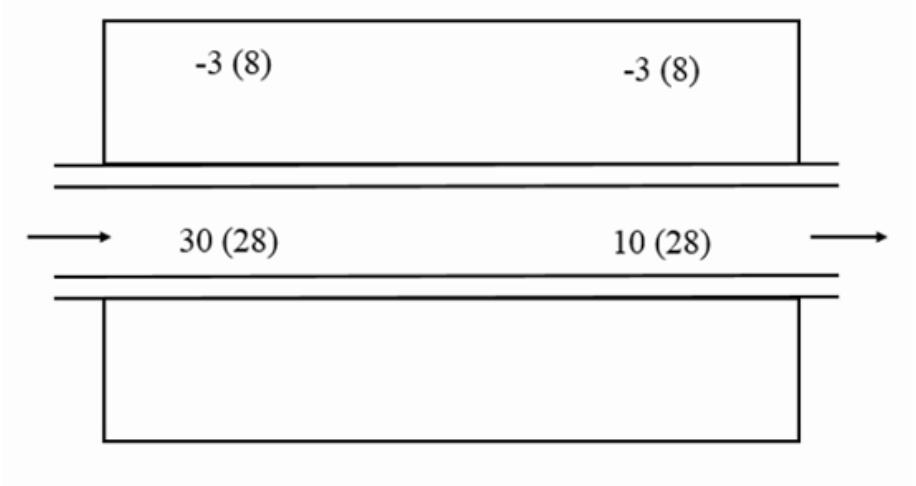

(a)

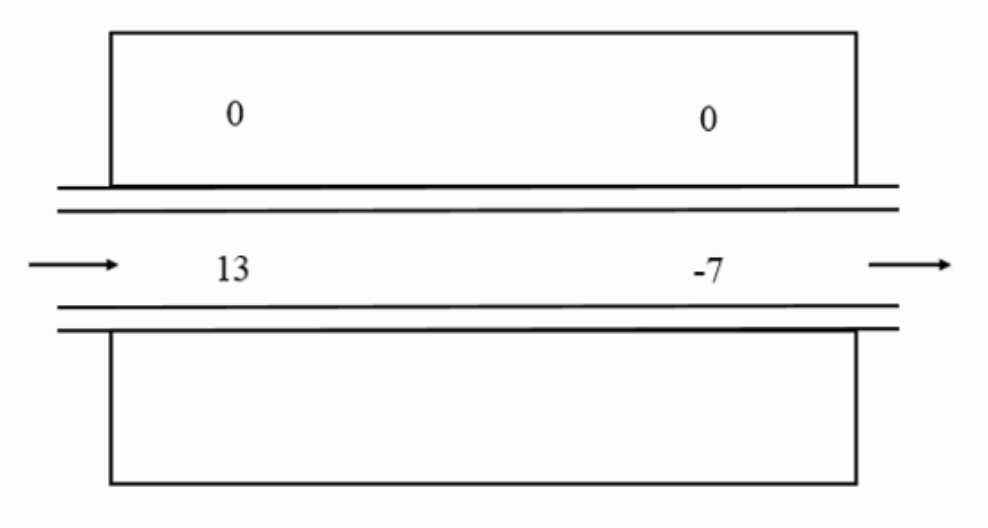

(b)

Figure 1.5 Schematic view of the pressures. The osmotic pressures which drive the flow into the capillary are shown within brackets in (a). The net transmembrane pressures are shown in (b). All pressures are in mm of Hg.

The osmotic pressure drop is 20 mm in both arteriole and venuole ends. If σ is set to be 1 (it is generally close to 1) and the effect of osmotic pressure is subtracted from the actual pressures, the transmembrane pressures that result are shown in Figure 1.5. The problem solved below cannot handle this many constraints. There the transmembrane osmotic pressure is set to zero and the difference between inlet and outlet pressures in a capillary is set to 20 mm.

1.5. PREVIEW

To understand the pharmacokinetics, it is necessary to understand the delivery of drugs, the distribution and the mass transfer of the drugs in the capillaries and extravascular tissues and in various organs (including tumors). As the drug is transported through the blood to the tissue or its target, it is very important to study the flow of plasma from the capillaries to the tissue, because the effective capillary wall is the only site that the drug can penetrate.

A common model for studying drug distribution is the stirred tank model described in Section 2.1, which does not consider any tissue mass transfer resistance (Baxter and Jain, 1995), although it takes into account the resistance of the capillary membrane. Therefore, it does not describe the actual concentration of drug in the extra-vascular space, the distribution within the organ. Another approach is that of Krogh cylindrical which deals with a single capillary to study the mass transfer from blood to extravascular tissue that takes place through the walls of the capillary (Krogh, 1919). Traditionally Krogh cylinder model considers diffusion rather than pressure-driven convective flow (Fournier, 1999). Some models consider convection due to lymph flow,

but the driving force for local convection is much higher (Jain, 1998). The next section will discuss these models. Implicit in the traditional present Krogh cylinder model is the feature that convection is small and can be neglected. Only diffusion of the drug is considered. Whereas convection is small in the tissues, the diffusion in tissues (below 10^{-5} cm^2/s, Saltzman, 2001) is also small and convection may not be neglected in comparison.

In the third section, the local convective flow and diffusion of the plasma in the interstitial space are discussed quantitatively, which improves the Krogh cylinder model. For a proper mass transfer calculations, a fluid flow model is first required. Eventually, there are plans to further carry out large-scale transport work. It is expected that the simple capillary effect can be summarized as an effect on the entire organ (Fournier, 1999).

2. PREVIOUS WORK

2.1. PHARMACOKINETIC MODEL

Pharmacokinetics studies the bioavailability of drugs, in which the drug is that is absorbed and eventually reaches the plasma. The concentration in plasma decreases over time as the drug is excreted through the kidneys or destroyed in the liver. As the drug concentration is a function of time, it will reach a very high level when ingested and then fall off. The integral under the curve is approximately related to bioavailability. There are many unknown factors in the therapeutic action. Therefore, bioavailability is considered as a measure of drug efficacy. In order to obtain sufficient bioavailability in treatment, sometimes the dose needs to be increased to the extent that it is harmful to the body. The clearance rate may also be high and result in low bioavailability, and then the concentration falls, perhaps it will be lower than the required level and have no therapeutic effect. The drugs cannot reach specific organs which need treatment, and drugs first reach other parts of the body such as the heart in large amounts causing damage. The general flow is shown in Figure 2.1. Material balance is satisfied, if the urinary excretion U is compensated by the same amount of liquid entering the box shown as plasma.

Every organ is further divided into two sub-compartments: the vascular space, and the extravascular space or the interstitial space as shown in Figure 2.2. There is a membrane that separates the two chambers and has the same properties as the membrane around the capillary tube. Q_i is total quantity plasma input, and C_{pl} is plasma in the capillary. L_i represents the flow to the lymphatic system which only happens to the fluid

that has left the vascular space for the interstitial space. The remaining fluid returns to the circulatory system.

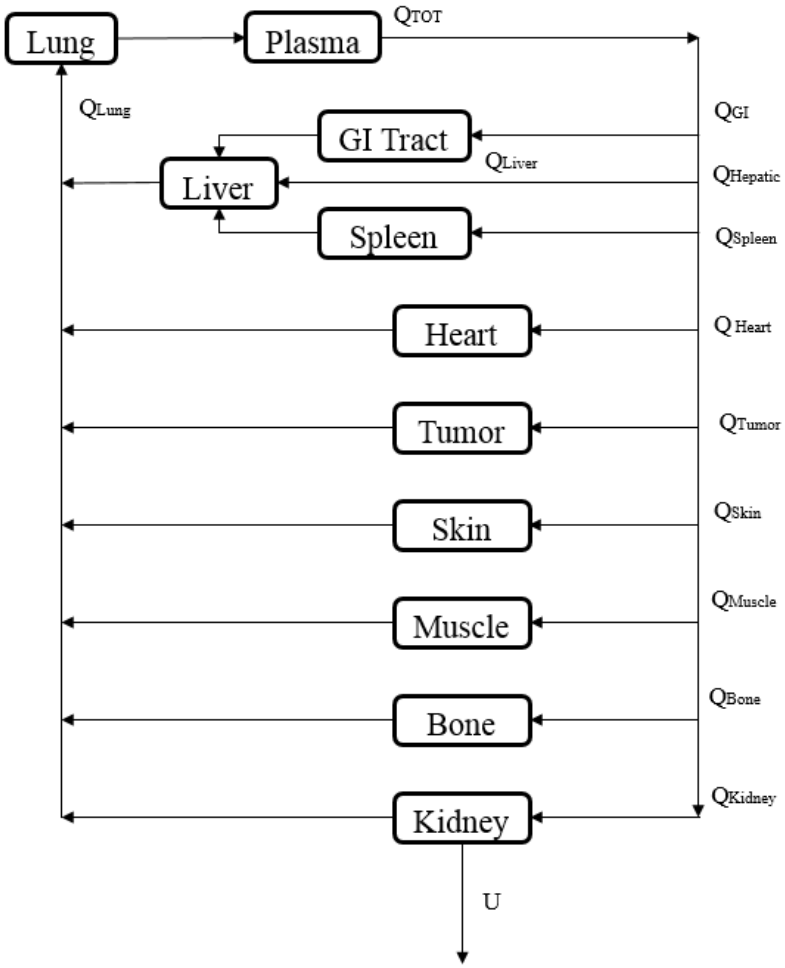

Figure 2.1 The Pharmacokinetic Model of the flow in the body (Sane, 2002).

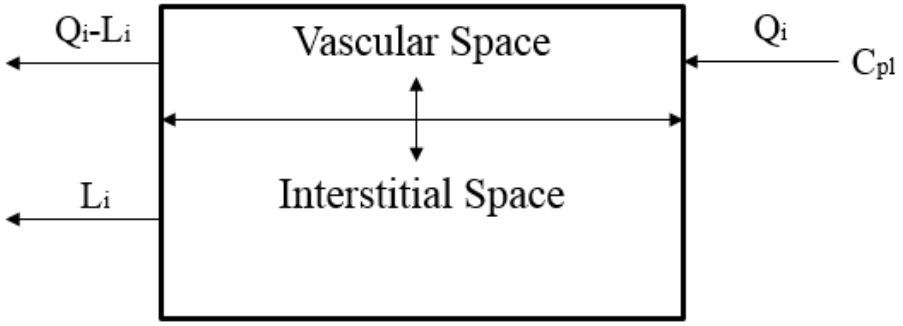

Figure 2.2 Vascular and extravascular sub-compartments (Sane, 2002).

2.2. KROGH CYLINDER MODEL

Capillaries are the main seat of mass transfer between blood and extravascular tissue. As mentioned earlier, their surface area is very large and their walls do not contain smooth muscle tissue. The capillary wall is permeable and obeys the phenomenology of membrane transport. In the model, only diffusion has so far been assumed to occur in extravascular tissue. However, flow is known to take place through the capillary walls, out of the capillary near the arterial end and the same flow returns at the venous end. Additional, the calculation by Starling showed a net average outflow of 28.3 mm and a net average inflow of 28 mm. These values are averages and not constants. The actual pressure of the capillary is very dynamic and varies locally. Almost of all the flow returns to the capillaries, except for a small fraction that is eventually absorbed by the lymphatic system. Therefore, according to Guyton and Hall (2000), 90 percent of the fluid that goes out through the membrane returns to it. The net outflow is to the lymph.

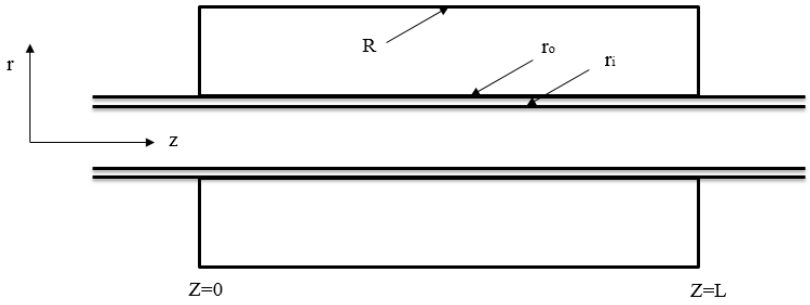

Figure 2.3 Schematic view of Krogh Cylinder.

2.3. PRESENT MODEL

The model used here considers only the fluid flow. The dimensions of the Krogh cylinder is considered in the Table 2.1 below. The organ under consideration is the liver and we also consider a typical tumor. From the point of view of fluid flow, the extravascular tissue is considered to be a porous medium of permeability k. The flow through the capillary tube is laminar. We also know the fraction of fluid entering that is lost to the lymphatic system.

The values of the vascular space and the interstitial space of an organ are known which ratio is the same as $r_i^2 / (R - r_i)^2$ in Figure 2.3. This way R can be calculated. Similarly L_i/Q_i in Figure 2.2 is ω.

Table 2.1 Dimensions of the Krogh Cylinder for Liver and Tumor.

L	Length of the capillary	0.02 cm	Healthy tissue	Netti et al (1996)
r_o	Outer radius of the capillary	0.00055 cm	Healthy tissue	Netti et al (1996)
L_p	Membrane hydraulic coefficient	2.700 x10^{-11} cm/(dyn.s)	Liver	Baxter and Jain (1989)
L_p	Membrane hydraulic coefficient	21.003x10^{-11} cm/(dyn.s)	Tumor tissue	Baxter and Jain (1989)
r_i	Inner radius of the capillary	0.0005 cm	Healthy tissue	Netti et al (1996)
μ	Viscosity of plasma	10^{-2} poise	Similar to water	Fournier (1999)
$\hat{\mu}$	Viscosity of blood in the capillary	3×10^{-3} poise	Whole blood	Fournier (1999)
Δp	Pressure drop	26664.4 dyn/cm^2	Healthy tissue	Guyton and Hall (2000)
$K= k/\mu$	Conductivity	6.398x10^{-12} cm^2/(dyn.s)	Liver	Swabb et al (1974)
$K= k/\mu$	Conductivity	2.250x10^{-10} cm^2/(dyn.s)	Tumor	Boucher et al (1998)
ω	Fraction fluid lost	5-10%	Tumor	Gullino and Grantham (1961)
ω	Fraction fluid lost	0.01%	Liver	Baxter, Zhu, Mackensen, and Jain (1994)

3. CONVECTIVE –DIFFUSIVE MODEL

3.1. KROGH CYLINDER MODEL

Krogh cylinder model for the tissue and convection are consider. Each capillary is assumed to supply blood to certain amount of tissue. The blood supplies to the space of tissue is determined by numerical values from literature. The basic model is that of Sane (2002) but contains many corrections and changes.

3.1.1. Model of the Flow in Capillary. The cross-section area is very small in capillary, the flow in capillaries lies in the low Reynolds number limit from Schmidt-Schonbein (1999) and which is applied here. The fluid motion is given by Stokes equation, and assumes the blood is Newtonian fluid. Hence, the momentum equation is

$$\mathbf{0} = -\nabla \hat{p} + \hat{\mu}\nabla^2 \hat{\boldsymbol{v}} \tag{3.1}$$

All quantities that refer to flow in the capillary are shown with carats. The continuity equation is

$$\nabla . \hat{\boldsymbol{v}} = 0 \tag{3.2}$$

3.1.2. Model for Flow through the Extravascular Space. In the extravascular space, the layout is considered to be spherical particles with interstices between them where the flow of fluid occurs. Fibrous polysaccharides and proteins fill in the interstices space between cells in which hider plasma flow. The equation could be described as the flow though the porous medium given by Brinkman (1947) equation

$$\mathbf{0} = -\nabla p + \mu\nabla^2 \boldsymbol{v} - \frac{\mu}{k}\boldsymbol{v} \tag{3.3}$$

where the k is the permeability, and it relates to the size and volume fraction. In Darcy's law equation the viscous term, the second term on the right-hand side is missing; **v** is superficial velocity in the interstices space, which is the inter-cellular space and filled with fibers.

The continuity equation is

$$\nabla . \boldsymbol{v} = 0 \tag{3.4}$$

Both can be combined to provide

$$0 = \mu E^4 \psi - \frac{\mu}{k} E^2 \psi \tag{3.5}$$

μ can be eliminated, and then equation will become

$$E^4 \psi = \frac{E^2 \psi}{k} \tag{3.6}$$

3.2. SOLUTION

In the porous medium, the flow is two dimensional: the radial velocity $v_r = \frac{1}{r}\frac{\partial \psi}{\partial z}$ and the axial velocity $v_z = -\frac{1}{r}\frac{\partial \psi}{\partial r}$ which represents to r and z, the two directions. The continuity and momentum equations are both satisfied by the solution to

$$\mathrm{E}^4 \psi = k \mathrm{E}^2 \psi \tag{3.7}$$

which can be written as

$$\mathrm{E}^2 \psi_1 = k \psi_1 \tag{3.8}$$

$$\mathrm{E}^2 \psi = k \psi_1 \tag{3.9}$$

where

$$\mathrm{E}^2 = \frac{\partial^2}{\partial r^2} - \frac{1}{r}\frac{\partial}{\partial r} + \frac{\partial^2}{\partial z^2} \;\; and \;\; k^{-\frac{1}{2}} = s \tag{3.10}$$

which the differential equation satisfied by the solution of Stokes stream function in cylinder coordinate. A change of variable to

$$\xi = sr, \zeta = sz, \text{ and } s = 1/\sqrt{k} \tag{3.11}$$

By using the method of separation of variables and $\psi_1 = P(\xi)X(\zeta)$ and Eq. (3.11) becomes

$$\xi\frac{X''}{X} = \frac{1}{\xi}\frac{P'}{P} - \frac{P''}{P} = -b^2 \tag{3.12}$$

and where P and Q are

$$P = c_3\xi I_1(\gamma\xi) + c_4\xi K_1(\gamma\xi) \tag{3.13}$$

$$X = c_1 cos(b\zeta) + c_2 sin(b\zeta) \tag{3.14}$$

where $\gamma^2 = 1 + b^2$, b is constant of separation, c_i are constants of integration. $I_1(\gamma\xi)$ is the modified Bessel function of the first kind, first order, and $K_1(\gamma\xi)$ is the modified Bessel function of the second kind, first order.

The solution for $\psi = Q(\xi)X(\zeta)$ from Eq. (3.9) is

$$\frac{\partial^2 Q}{\partial \xi^2} - \frac{1}{\xi}\frac{\partial Q}{\partial \xi} + b^2 Q = P \tag{3.15}$$

Separate Q to $U_0 + U_1$

$$Q = U_0 + U_1 \tag{3.16}$$

where U_0 is the complimentary solution

$$U_0 = c_5 I_0(b\xi) + c_6 K_0(b\xi) \tag{3.17}$$

and the particular integral is

$$\frac{\partial^2 U_1}{\partial \xi^2} - \frac{1}{\xi}\frac{\partial U_1}{\partial \xi} - b^2 U_1 = P \tag{3.18}$$

With $\gamma^2 = 1 + b^2$ the solution is

$$U_1 = P \tag{3.19}$$

So

$$Q = c_5 I_0(b\xi) + c_6 K_0(b\xi) + P \tag{3.20}$$

Hence the stream function is

$$\begin{aligned}\psi = {} & \big(c_3 \xi I_1(\gamma\xi) + c_4 \xi K_1(\gamma\xi) + c_5 \xi I_1(b\xi) + c_6 \xi K_1(b\xi)\big)\big(c_1 cos(b\zeta) + c_2 sin(b\zeta)\big) \\ & + \left(\alpha_3 \xi I_1(\xi) + \alpha_4 \xi K_1(\xi) + \alpha_5 \frac{\xi^2}{2} + \alpha_6\right)(\alpha_1 \zeta + \alpha_2)\end{aligned} \tag{3.21}$$

In the interstitial fluid, the velocity both Z and R direction, and pressure present

$$\begin{aligned}v_z = {} & -s^2[c_3 \gamma I_0(\gamma\xi) - c_4 \gamma K_0(\gamma\xi) + c_5 b I_0(b\xi) - c_6 b K_0(b\xi)][c_1 b cos(b\zeta) \\ & + c_2\, sin(b\zeta)] - s^2[\alpha_3 I_0(\xi) - \alpha_4 K_0(\xi) + \alpha_5][\alpha_1 \zeta + \alpha_2]\end{aligned} \tag{3.22}$$

$$\begin{aligned}v_r = s^2 \Big\{ & [c_3 I_1(\gamma\xi) + c_4 K_1(\gamma\xi) + c_5 I_1(b\xi) + c_6 K_1(b\xi)][c_2 b cos(b\zeta) - c_1 b\, sin(b\zeta)] \\ & + \alpha_1 \left[\alpha_3 I_1(\xi) + \alpha_4 K_1(\xi) + \alpha_5 \frac{\xi}{2} + \frac{\alpha_6}{\xi}\right]\Big\}\end{aligned} \tag{3.23}$$

$$\begin{aligned}\frac{\wp}{s^3 \mu} = {} & [c_5 I_0(b\xi) - c_6 K_0(b\xi)][c_1\, sin(b\zeta) - c_2 cos(b\zeta)] + \alpha_5 \left[\alpha_1 \frac{\zeta^2}{2} + \alpha_2 \zeta\right] \\ & - \alpha_1 \left[\alpha_5 \frac{\xi^2}{4} + \alpha_6 ln\xi\right] + \alpha_7\end{aligned} \tag{3.24}$$

Inside the capillary, a general solution for the stream function is available for a Newtonian fluid (Haberman and Sayre, 1958). Unlike in the extravascular tissue, which is a porous solid, the space in the capillary is a void; but unlike the fluid that flows in the tissues, which is plasma, the fluid inside the capillary is whole blood and non-Newtonian and very inhomogeneous at these length scales. Nevertheless, we make the simplifying

assumption that the fluid is Newtonian and use the solution given by Haberman and Sayre (1958). It is noteworthy that their method of obtaining the stream function has been followed in obtaining the solution for the porous medium. All quantities in the capillary have been shown with carats. Solving these equations as before gives the solution as

$$\hat{\psi} = [\hat{c}_3\xi I_1(a\xi) + \hat{c}_4\xi K_1(a\xi) + \hat{c}_5\xi^2 I_0(a\xi) + \hat{c}_6\xi^2 K_0(a\xi)][\hat{c}_1 cos(a\zeta) + \hat{c}_2 sin(a\zeta)] + (\hat{\alpha}_3 + \hat{\alpha}_4\xi^2)(\hat{\alpha}_1 + \hat{\alpha}_2\zeta) + \hat{\alpha}_7\xi^4(\hat{\alpha}_5 + \hat{\alpha}_6\zeta) + \zeta^2(\hat{\alpha}_8\xi^2 + \hat{\alpha}_9\zeta + \hat{\alpha}_{10}) \quad (3.25)$$

$$\hat{v}_z = s^2\{[\hat{c}_4 aK_0(a\xi) - \hat{c}_3 aI_0(a\xi) - \hat{c}_5 a\xi I_1(a\xi) - 2\hat{c}_5 I_0(a\xi) + \hat{c}_6 a\xi K_1(a\xi) - 2\hat{c}_6 K_0(a\xi)][\hat{c}_1 cos(a\zeta) - \hat{c}_2 sin(a\zeta)] - 2\hat{\alpha}_4(\hat{\alpha}_1 + \hat{\alpha}_2\zeta) - 4\hat{\alpha}_7\xi^2(\hat{\alpha}_5 + \hat{\alpha}_6\zeta) - 2\hat{\alpha}_8\zeta^2\} \quad (3.26)$$

$$\hat{v}_r = s^2\left\{a[\hat{c}_3 I_1(a\xi) + \hat{c}_4 K_1(a\xi) + \hat{c}_5\xi I_0(a\xi) + \hat{c}_6\xi K_0(a\xi)][\hat{c}_2 cos(a\zeta) - \hat{c}_1 sin(a\zeta)] + \hat{\alpha}_2\left(\frac{\hat{\alpha}_3}{\xi} + \hat{\alpha}_4\xi\right) + \hat{\alpha}_6\hat{\alpha}_7\xi^3 + 2\zeta\left(\hat{\alpha}_8\xi + \frac{3\hat{\alpha}_9\zeta}{2\xi} + \hat{\alpha}_{10}\right)\right\} \quad (3.27)$$

$$\frac{\hat{\wp}}{s^3\mu} = 2a[\hat{c}_5 I_0(a\xi) + \hat{c}_6 K_0(a\xi)][\hat{c}_2 cos(a\zeta) - \hat{c}_1 sin(a\zeta)] + \hat{c}_7 - 4\hat{\alpha}_6\hat{\alpha}_7\xi^2 - 16\hat{\alpha}_7\left(\hat{\alpha}_5\zeta + \hat{\alpha}_6\frac{\zeta^2}{2}\right) + 6\hat{\alpha}_9 ln\xi + 4\hat{\alpha}_8\zeta + \hat{\alpha}_{11} \quad (3.28)$$

3.3. BOUNDARY CONDITIONS

The boundary conditions are applied in Krogh cylinder:

There is no slip at each capillary walls

1. $v_Z = 0 \; at \; \zeta = 0$
2. $v_Z = 0 \; at \; \zeta = \Lambda = sL$

The leak of the capillary

3. $\int_0^{\Lambda} v_r\,|_{\xi=Z} 2\pi Z\, d\zeta = \omega\langle \hat{V}_{zo}\rangle \pi Z^2$ at $\xi = Z = sR$
4. $v_z = 0$ at $\xi = \xi_0 = sr_o$
5. $v_z = 0$ at $\xi = Z = sR$

Inlet velocity of plasma in capillary

6. $\hat{v}_z|_{\zeta=0} = 2\langle \hat{v}_{zo}\rangle \left[1 - \left(\frac{\xi}{\xi_i}\right)^2\right]\ at\ \zeta = 0$

Outlet velocity of plasma in capillary

7. $\hat{v}_z|_{\zeta=\Lambda} = (1-\omega) \times 2\langle \hat{v}_{zo}\rangle \left[1 - \left(\frac{\xi}{\xi_i}\right)^2\right]\ at\ \zeta = \Lambda$

The center line of fluid in capillary

8. $\hat{v}_z$ is finite at $\xi = 0$
9. $\hat{v}_r = 0$ at $\xi = 0$
10. $\hat{v}_z = 0$ at $\xi = \xi_i = sr_i$

The fluid pressure and osmotic pressure force at the capillary

11. $\hat{v}_r|_{\xi_i} = L_P\left(\hat{\wp}|_{\xi_i} - \wp|_{\xi_0} - \sigma\Delta\Pi\right)$

The fluid permeate from capillary to tissue

12. $2\pi\xi_i \hat{V}_r|_{\xi_i} = 2\pi\xi_0 v_r|_{\xi_0}$

Applying the boundary conditions a set of the linear equations are obtained which are solved simultaneously for the constants. The overall conservation requires that the constant $c_2 c_3 = 0$. To satisfy conditions 8 and 12, the Fourier sine and cosine series are needed

$$\frac{\zeta}{\Lambda}-\frac{\zeta^2}{\Lambda^2}=\frac{8}{\pi^3}\sum_{m=0}^{\infty}\frac{sin(2m+1)\pi\frac{\zeta}{\Lambda}}{(2m+1)^3} \qquad 0\le\zeta\le\Lambda \tag{3.29}$$

$$\left(\frac{\pi\zeta}{\Lambda}\right)^2=\frac{\pi^2}{3}-4\sum_{n=1}^{\infty}(-1)^{n+1}\frac{cos\left(\frac{n\pi\zeta}{\Lambda}\right)}{n^2} \qquad 0\le\zeta\le\Lambda \tag{3.30}$$

$$\frac{\zeta}{\Lambda}-\frac{1}{2}=\frac{4}{\pi^2}\sum_{n=1}^{\infty}-\frac{cos(2m+1)\pi\frac{\zeta}{\Lambda}}{(2m+1)^2} \qquad 0\le\zeta\le\Lambda \tag{3.31}$$

Appendix A has all the details on how the set of equations that are found and solved.

These constants are seen in the final equations listed below.

$$\frac{v_Z}{\langle\hat{v}_{zo}\rangle}=\beta\sum_{m=1}^{\infty}sin(a_n\zeta)\left[c_{2n}c_{4n}\gamma_nK_0(\gamma_n\xi)-c_{2n}c_{5n}a_nI_0(a_n\xi)+c_{2n}c_{6n}a_nK_0(a_n\xi)\right] \tag{3.32}$$

$$\frac{v_r}{\langle\hat{v}_{zo}\rangle}=\beta\sum_{m=1}^{\infty}a_n\,cos(a_n\zeta)[c_{2n}c_{4n}K_1(\gamma_n\xi)+c_{2n}c_{5n}I_1(a_n\xi)+c_{2n}c_{6n}K_1(a_n\xi)] \tag{3.33}$$

$$+\frac{\omega{\xi_i}^2}{2\Lambda}\frac{1}{\xi}$$

$$\frac{\wp}{\Delta\wp}=\alpha\sum_{m=1}^{\infty}cos(a_n\zeta)\left[-c_{2n}c_{5n}I_0(a_n\xi)+c_{2n}c_{6n}K_0(a_n\xi)\right] \tag{3.34}$$

$$\frac{\psi}{\langle\hat{v}_{zo}\rangle{\xi_i}^2}=\beta\sum_{m=1}^{\infty}sin(a_n\zeta)\frac{\xi}{{\xi_i}^2}[c_{2n}c_{4n}K_1(\gamma_n\xi)+c_{2n}c_{5n}I_1(a_n\xi)+c_{2n}c_{6n}K_1(a_n\xi)] \tag{3.35}$$

$$+\frac{\omega{\xi_i}^2}{2\Lambda}\frac{1}{\xi}$$

$$\frac{\hat{v}_z}{\langle\hat{v}_{zo}\rangle}=\beta\sum_{m=1}^{\infty}-sin(a_n\zeta)\left[\hat{c}_{2n}\hat{c}_{3n}a_nI_0(a_n\xi)+\hat{c}_{2n}\hat{c}_{5n}a_n\xi I_1(a_n\xi)\right. \tag{3.36}$$

$$\left.+2\hat{c}_{2n}\hat{c}_{5n}I_0(a_n\xi)\right]+2\left(1-\frac{\xi^2}{{\xi_i}^2}\right)-2\omega\frac{\zeta}{\Lambda}\left(\frac{\xi^2}{{\xi_i}^2}-\frac{\zeta}{\Lambda}\right)$$

$$\frac{\hat{v}_r}{\langle \hat{v}_{zo} \rangle} = \beta \sum_{m=1}^{\infty} a_n cos(a_n \zeta)[\hat{c}_{2n}\hat{c}_{3n} I_1(a\xi) + \hat{c}_{2n}\hat{c}_{5n}\xi I_0(a_n \xi)] + \frac{\omega}{\Lambda}\xi\left(1 - \frac{1}{2}\frac{\xi^2}{{\xi_i}^2}\right) + \beta \frac{\xi}{(2\alpha + \xi_i)}\left(\frac{1}{2} - \frac{\zeta}{\Lambda}\right) \tag{3.37}$$

$$\frac{\hat{\wp}}{\Delta\wp} = 2\alpha \sum_{m=1}^{\infty} cos(a_n \zeta) a_n \hat{c}_{2n}\hat{c}_{5n} I_0(a_n \xi) - \left[\frac{\xi_i + 12\alpha}{\xi_i + 6\alpha}\right]\frac{\zeta}{\Lambda} \tag{3.38}$$

$$\frac{\hat{\psi}}{\langle \hat{v}_{zo} \rangle {\xi_i}^2} = \beta \sum_{m=1}^{\infty} sin(a_n \zeta)\,[\hat{c}_{2n}\hat{c}_{3n}\xi I_1(a_n \xi) + \hat{c}_{2n}\hat{c}_{5n}\xi^2 I_0(a_n \xi)] + \beta \frac{\zeta \xi^2}{2(\xi_i + 2\alpha)}\left(1 - \frac{\zeta}{\Lambda}\right) - \left(\frac{\xi}{\xi_i}\right)^2\left(1 - \frac{1}{2}\frac{\xi^2}{{\xi_i}^2}\right) \tag{3.39}$$

where n = 2m-1

$$\alpha = L_p s \mu \tag{3.40}$$

$$\beta = \frac{L_p \Delta\wp}{\langle \hat{V}_{zo} \rangle} \tag{3.41}$$

$$\gamma_n = \sqrt{{a_n}^2 + 1} \tag{3.42}$$

$$a_n = \frac{\pi n}{\Lambda} \tag{3.43}$$

$$\mu_r = \frac{\hat{\mu}}{\mu} \tag{3.44}$$

4. RESULTS AND DISCUSSION

4.1. LENGTH SCALES AND DIMENSIONLESS GROUPS

The equations describing the flow profiles contain four length scales: $k^{1/2}$, r_i, r_o , and L . The last three are similar in magnitude, but the first is very different and of the order of 1-10 nm, which gives an estimate of gap width between the cells, that is, the interstitial spaces in the extravascular tissue. Because of this disparity, the dimensionless term Z works out to a very large number, in tens of thousands. As a result, some of the Bessel functions with such arguments become too high to accommodate in any computer program. It also shows why numerical solution was avoided. $k^{1/2}$ gives us very stiff equations which are difficult to solve with accuracy. Eventually such terms were set to infinity and the condition of boundedness was imposed making the constant c_3 in Eq. (3.22) to be zero.

Two other dimensionless groups α, and β, Eqs. (3.40) and (3.41), play key roles. Most of the flow in the porous medium is governed by Darcy's law, Eq. (3.3) without the second term on the right. In that case, velocity ~ $(k/\mu)\,\Delta p$ (length scale). The length scale is taken to be the interstitial dimension $k^{1/2}$ (= s^{-1}), in which case the resistance to flow in the porous medium Δp/velocity ~ μs. The resistance to flow through the capillary wall is ~ $1/L_p$. This leads to the conclusion that

$$\alpha = \frac{\text{resistance to flow in the porous medium}}{\text{resistance to flow across the capillary wall}} = L_p s \mu \qquad (4.1)$$

$$\beta = \frac{\text{resistance to flow through the capillary}}{\text{resistance to flow across the capillary wall}} = \frac{L_p \Delta \wp}{\langle \hat{v}_z \rangle} \tag{4.2}$$

The values of individual constants making up α and β and the four length scales have been taken from the compilations in (Netti, et al,1996 and Baxter and Jain, 1989). If we use these values then

$$s = 1.4 \times 10^6 \, cm^{-1} \tag{4.3}$$

which the numerical routines of MATLAB cannot handle and hence s has been decreased to 10^6. Further, the calculated values of other constants lead to

$$\alpha = 8.100 \times 10^{-7} \text{ and } \beta = 5.184 \times 10^{-7} \tag{4.4}$$

These are referred to as micro-constants.

As mentioned earlier we set ΔΠ to zero and assume a value for the inlet velocity $< \hat{v}_{z0} >$. At the end of the calculations, we calculate the pressure drop across the capillary as $\Delta \hat{\wp} = \hat{\wp}\big|_{z=0} - \hat{\wp}\big|_{z=L}$. Because all equations are linear, we set $\Delta \wp$ to 20 mm and find proportionately the corresponding value of $< \hat{v}_{z0} >$. This is done where the organ (liver or tumor) and the value of ω has been fixed beforehand.

4.2. FIGURES OF VELOCITY AND PRESSURE

The expressions of the integral constant in the solution are very complex and consists of a large number of products of five Bessel functions. Boundary conditions selected allow for leaky issues (ω not equal to zero), which is the lymph circulatory system. Using MATLAB to calculate the constants of these expressions to get the graphics, the program is very slow and report that matrix is close to singular or badly

scaled due to 5×5 Bessel functions. In MATLAB, the five equations obtained under the boundary conditions are directly solved, and the constant values are obtained. In Sane (2002)'s thesis, her conclusion mention that the microvalues of α and β represent the relative resistances to flow and that is the blood zips through the capillary with very little plasma flowing out of the capillary membrane to extravascular tissue. The above conclusion also match with this report and the introduction mentions.

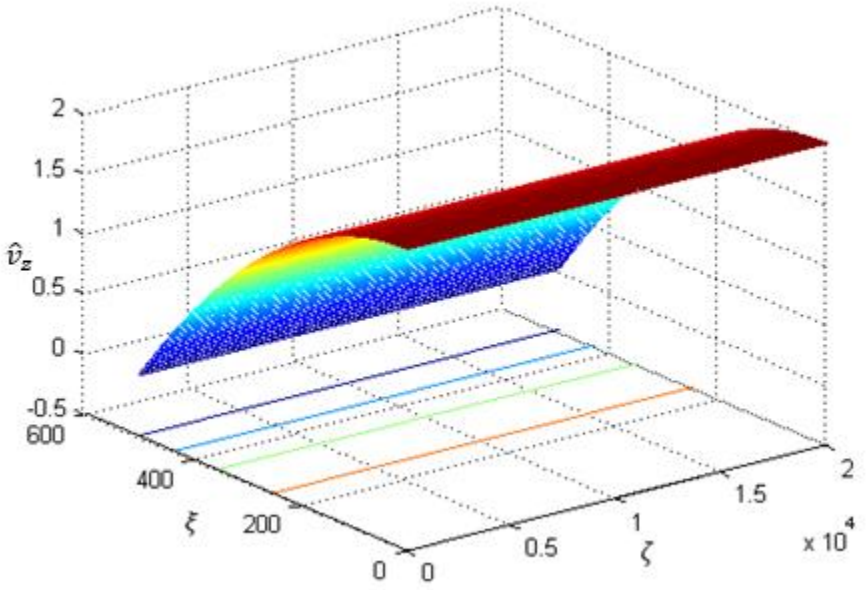

Figure 4.1 Axial velocity in the capillary in normal liver at ω = 0.

All the velocities in Figure 4.1 - Figure 4.4 and Figure 4.9 - Figure 4.12 are in centimeters pre-second, Figure 4.5, Figure 4.6, Figure 4.13, Figure 4.14 are stream functions, and Figure 4.7, Figure 4.8, Figure 4.15, Figure 4.16 pressures in dynes/cm^2. The axial velocity in the capillary is very high at ~ 1 cm/s. On the other hand the velocities in the extravascular tissue is ~ 10^{-13} cm/s, a very low value. However, a

circulation is observed in the extravascular tissue as anticipated. The leaky system is considered below for a tumor with ω = 0.1. The consequence of adding a leakage in the tumor leads to

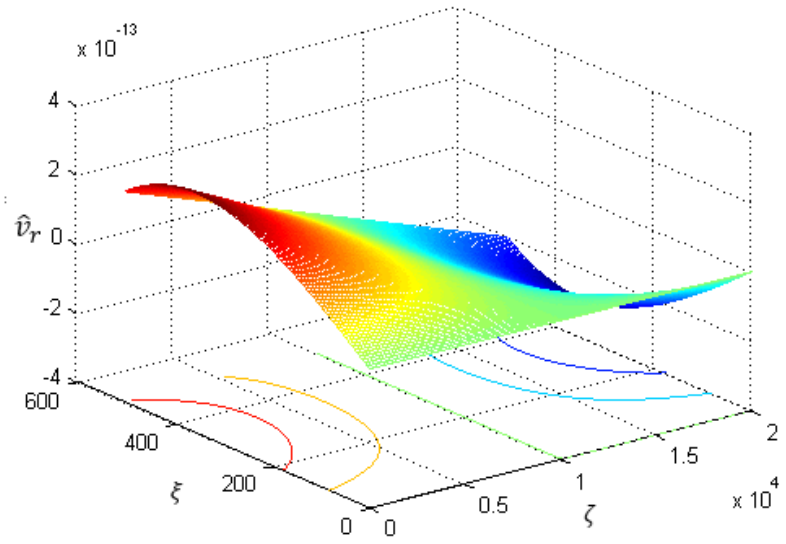

Figure 4.2 Radial velocity in the capillary in normal liver at ω = 0.

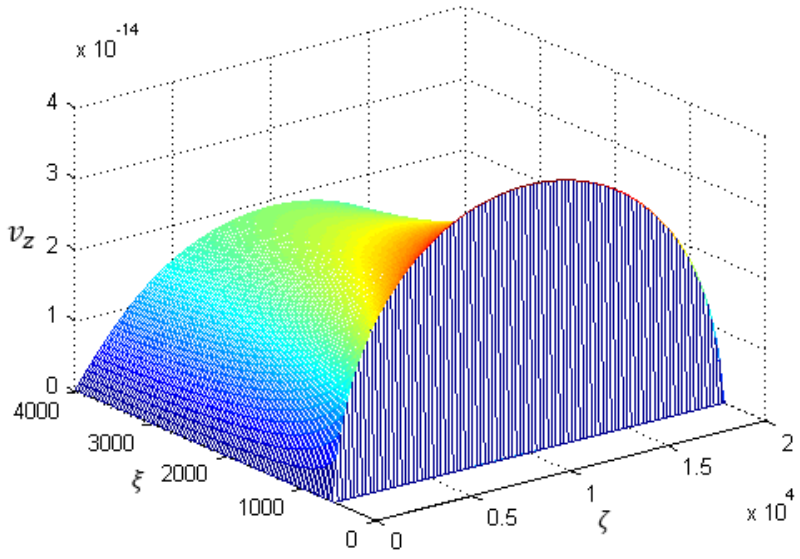

Figure 4.3 Axial velocity in the extravascular space in a normal liver for ω = 0.

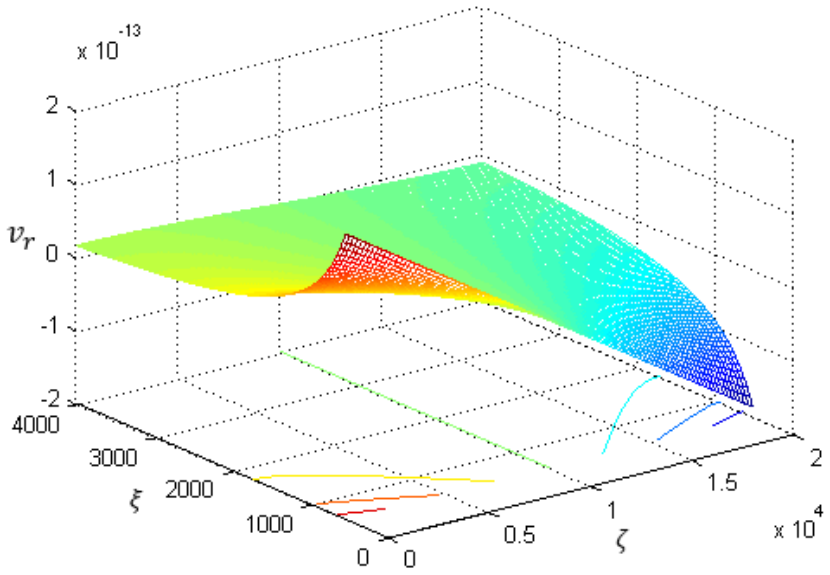

Figure 4.4 Radial velocity in the extravascular space in a normal liver at ω = 0.

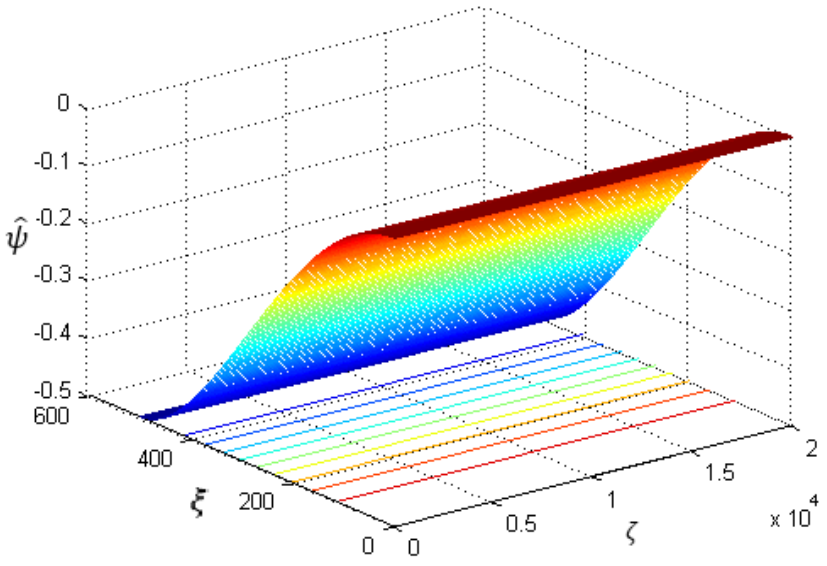

Figure 4.5 Stream function in the capillary in normal liver at ω = 0.

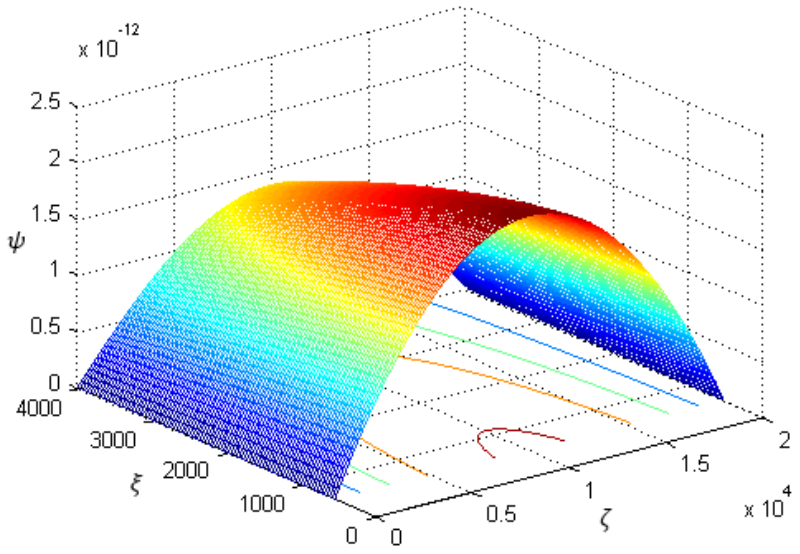

Figure 4.6 Stream function in the extravascular space in a normal liver at ω = 0.

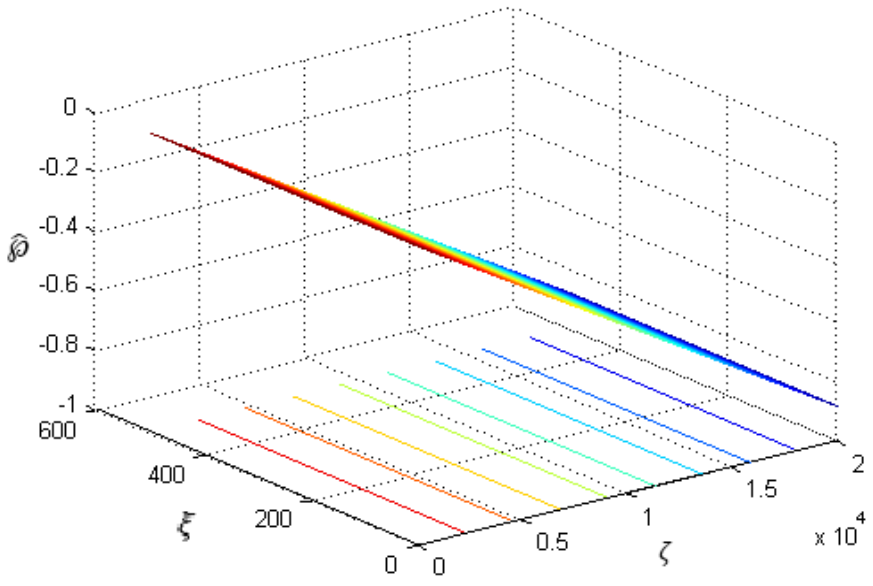

Figure 4.7Pressure in the capillary in normal liver at ω = 0.

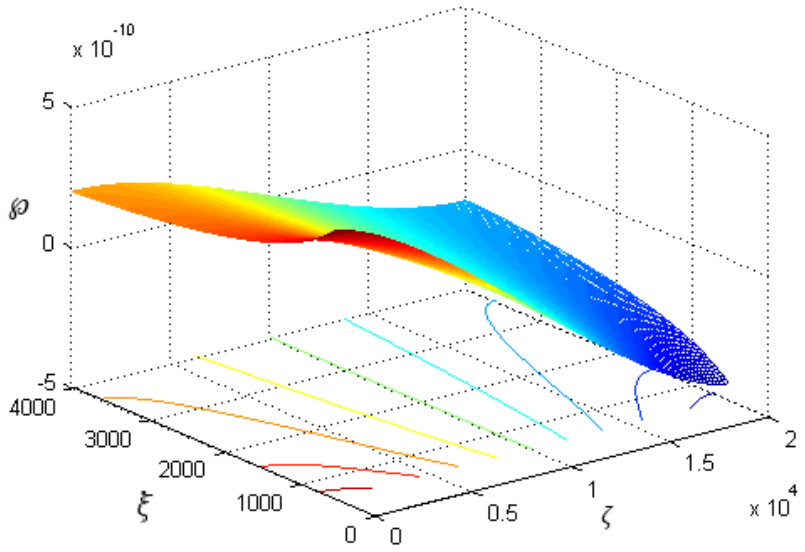

Figure 4.8 Pressure in the extravascular space in a normal liver at ω = 0.

virtual washout in the extravascular tissue. However, the axial velocity in the capillary still remains at ~ 1 cm/s. If ω is as low as 10^{-4} as in the healthy tissue, we will not see such a washout.

Whereas all numbers appear reasonable, one number of the axial velocity in the capillary is too high which is $< \hat{v}_{z0} > \sim 1$ cm/s, when it should be 0.02-0.17 cm/s (Aaron and James, 2015). $\Delta \hat{\wp} = \hat{\wp}\big|_{z=0} - \hat{\wp}\big|_{z=L}$ is kept at 20 mm of mercury as stated. This normalization is done for ω = 0. For ω greater than zero, this pressure drop falls linearly with increasing ω by not by much.

The consequence of the present results is that we can now look at convective-diffusive transport in Krogh cylinder next, using the velocity profiles obtained here. It is noteworthy that a big difference could be anticipated in "bioavailability" which is drug in the capillary and the amount of drug available in the extravascular tissue.

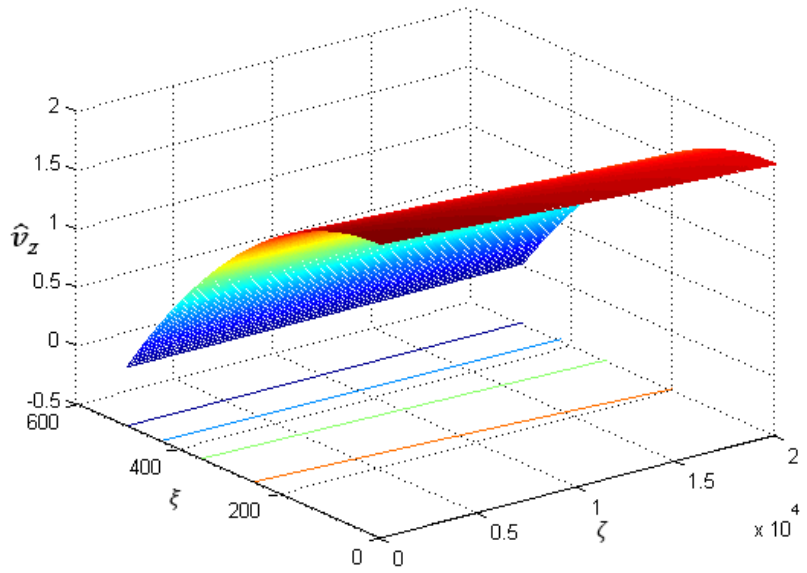

Figure 4.9 Axial velocity in the capillary in a tumor at ω = 0.1.

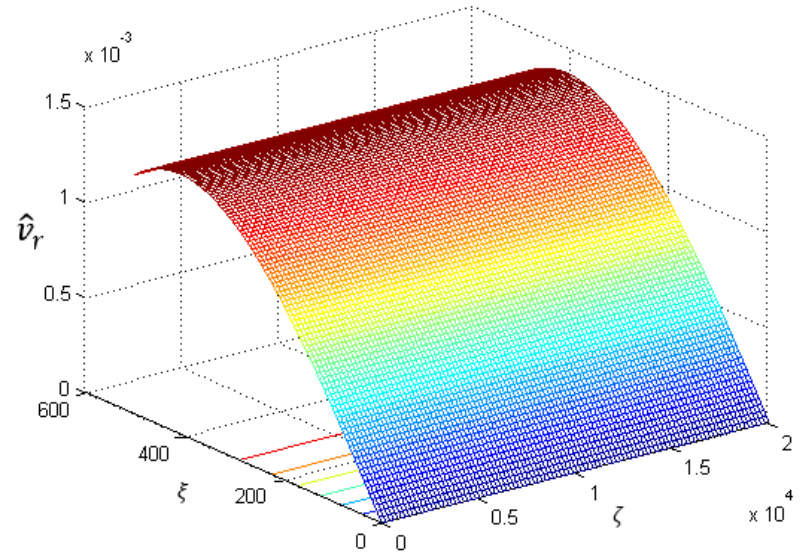

Figure 4.10 Radial velocity in the capillary in a tumor at ω = 0.1.

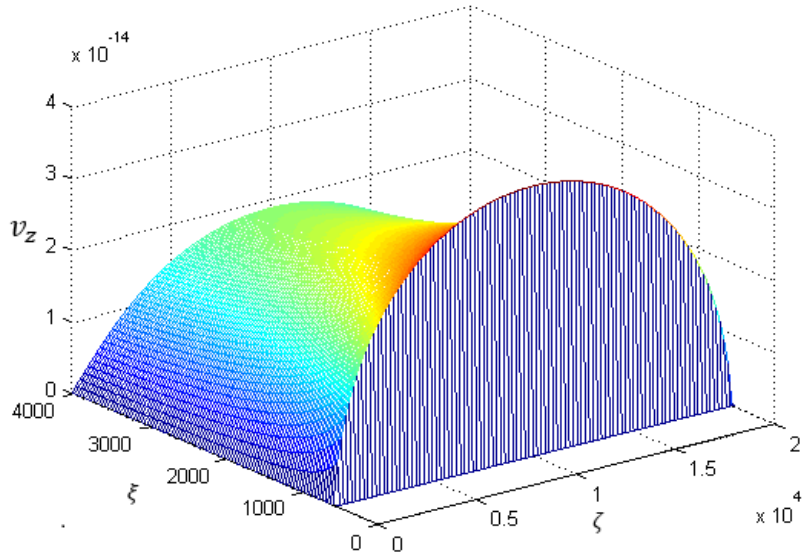

Figure 4.11 Axial velocity in the extravascular tissue in a tumor at ω = 0.1.

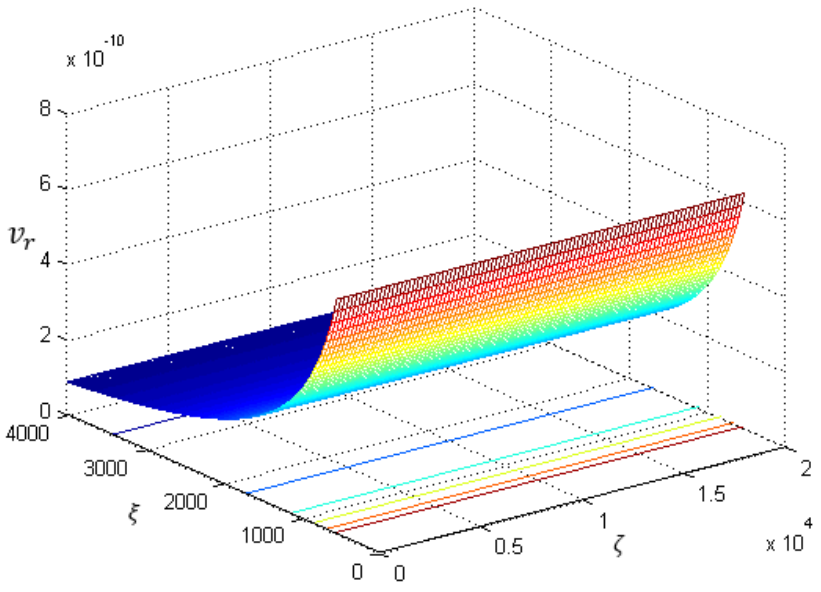

Figure 4.12 Radial velocity in the extravascular tissue in a tumor with ω = 0.1.

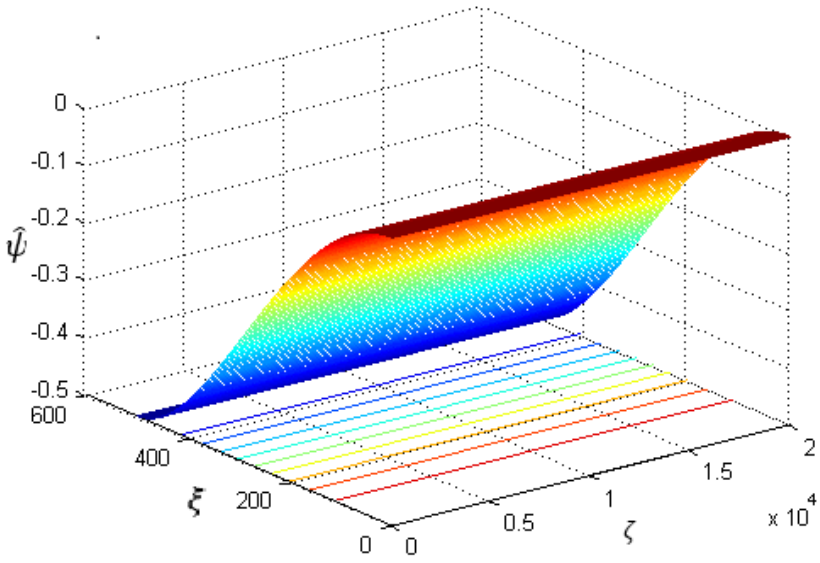

Figure 4.13 Stream function in the capillary in a tumor at ω = 0.1.

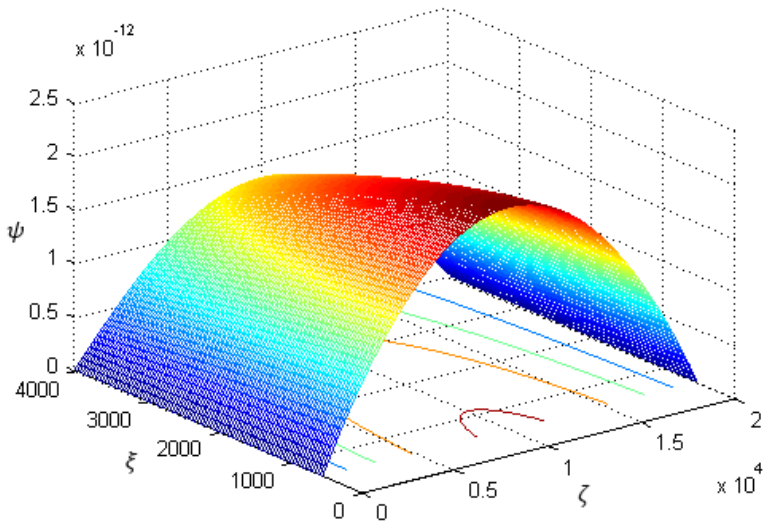

Figure 4.14 Stream function in the extravascular tissue in a tumor at ω = 0.1.

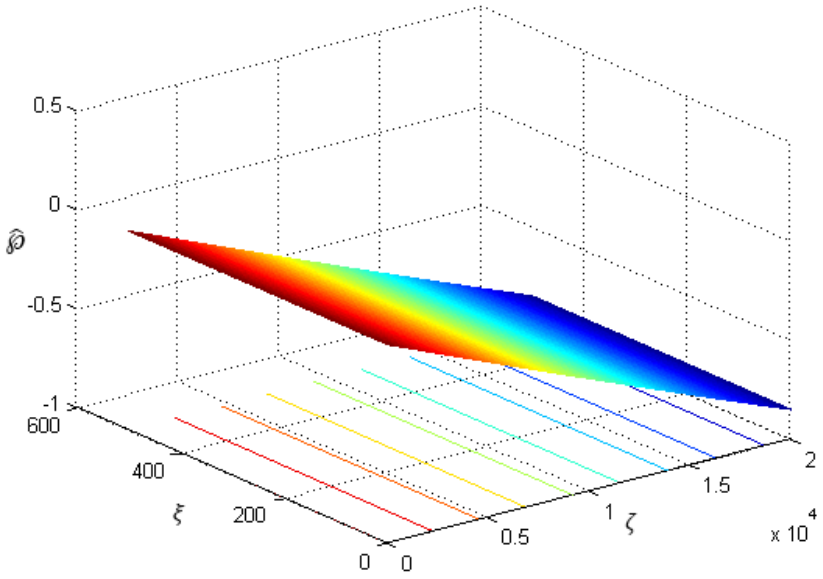

Figure 4.15 Pressure in the capillary in a tumor with ω = 0.1.

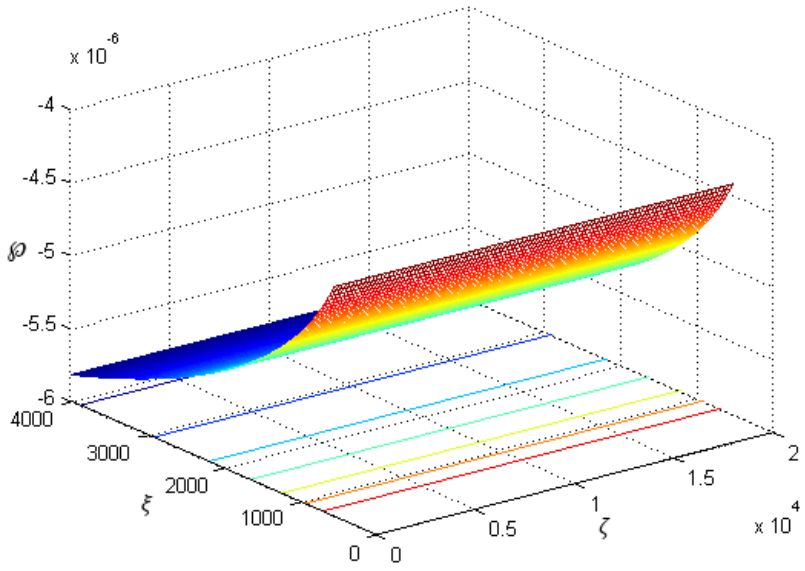

Figure 4.16 Pressure in the extravascular tissue in a tumor with ω = 0.1.

5. CONCLUSION

The main feature of the present results is that there is the mixing with capillary flow and extravascular tissue.

The convection has been accounted for in a Krogh cylinder using all measured parameters. Each capillary is assumed to supply plasma to certain amount of tissue. In an organ, all of these can be added in parallel to account for the entire organ. Convection appears to be very important in tumors (neoplastic tissues), its present but very low in healthy organs.

APPENDIX A.

APPLYING THE BOUNDARY CONDITIONS TO OBTAIN A SET OF FIVE LINEAR SIMULANEOUS EQUATIONS

BC 1 and BC 2 give

$$c_1 = 0, \tag{A-1}$$

$$\alpha_3 = \alpha_4 = \alpha_5 = 0 \tag{A-2}$$

BC 3 gives

$$\alpha_1\alpha_6 = \frac{\omega\langle\hat{V}_{zo}\rangle\xi_i^{\,2}}{2\Lambda s^2} \tag{A-3}$$

BC 4 gives

$$c_{2n}c_{3n}\gamma I_0(\gamma\xi_0) - c_{2n}c_{4n}\gamma K_0(\gamma) + c_{2n}c_{5n}bI_0(b\xi_0) - c_{2n}c_{6n}bK_0(b\xi_0) = 0 \tag{A-4}$$

BC 5 gives

$$c_{2n}c_{3n}\gamma I_0(\gamma Z) - c_{2n}c_{4n}\gamma K_0(\gamma Z) + c_{2n}c_{5n}bI_0(bZ) - c_{2n}c_{6n}bK_0(bZ) = 0 \tag{A-5}$$

BC 6 gives

$$\hat{\alpha}_1\hat{\alpha}_4 = -\frac{\langle\hat{V}_{zo}\rangle}{s^2} \tag{A-6}$$

$$\hat{\alpha}_5\hat{\alpha}_7 = \frac{1}{2}\frac{\langle\hat{V}_{zo}\rangle}{\xi_i^{\,2}s^2} \tag{A-7}$$

BC 7 gives

$$\hat{\alpha}_2\hat{\alpha}_4 + \hat{\alpha}_8\Lambda = \frac{\omega\langle\hat{V}_{zo}\rangle}{s^2\Lambda} \tag{A-8}$$

$$\hat{\alpha}_6\hat{\alpha}_7 = -\frac{1}{2}\frac{\omega\langle\hat{V}_{zo}\rangle}{\xi_i^{\,2}s^2\Lambda} \tag{A-9}$$

BC 8 gives

$$\hat{c}_{6n} = 0 \tag{A-10}$$

BC 9 gives

$$\hat{c}_{4n} = 0 \tag{A-11}$$

$$\hat{\alpha}_3 = \hat{\alpha}_9 = \hat{\alpha}_{10} = 0 \tag{A-12}$$

BC 10 gives

$$[\hat{c}_{2n}\hat{c}_{3n}aI_0(a\xi_i) + \hat{c}_{2n}\hat{c}_{5n}a\xi I_1(a\xi_i) + 2\hat{c}_{2n}\hat{c}_{5n}I_0(a\xi_i)]\sin(a_n\zeta) = -2\hat{\alpha}_8\Lambda^2\left(\frac{\zeta}{\Lambda} - \frac{\zeta^2}{\Lambda^2}\right) \tag{A-13}$$

Comparing equation A-13 and the Fourier sine series in equation 3.30

$$[\hat{c}_{2n}\hat{c}_{3n}aI_0(a\xi_i) + \hat{c}_{2n}\hat{c}_{5n}a\xi I_1(a\xi_i) + 2\hat{c}_{2n}\hat{c}_{5n}I_0(a\xi_i)] = \frac{-16(1-(-1)^n)\hat{\alpha}_8\Lambda^2}{\pi^3 2n^3} \tag{A-14}$$

BC 11 gives

$$[a\{\hat{c}_2\hat{c}_3I_1(a\xi_i) + (\xi_i - 2\alpha)\hat{c}_2\hat{c}_5I_0(a\xi_i)\} + \alpha\{-c_2c_5I_0(b\xi_0) + c_2c_6K_0(b\xi_0)\}]s^2\cos\left(\frac{n\pi\zeta}{\Lambda}\right) = -8\alpha s^2\hat{\alpha}_6\hat{\alpha}_7\zeta^2 - (4\alpha s^2\hat{\alpha}_8 + L_P\Delta\wp - 2s^2\hat{\alpha}_8\xi_i)\zeta + \left[\alpha s^2(\hat{c}_7 + \hat{\alpha}_{11}) - 4\alpha s^2{\xi_i}^2\hat{\alpha}_6\hat{\alpha}_7 - \alpha s^2\alpha_7 + s^2\xi_i\hat{\alpha}_8\Lambda - L_P\sigma\Delta\Pi\right] \tag{A-15}$$

We can have the sample formula

$$[\mathrm{a}\{\hat{c}_2\hat{c}_3 I_1(a\xi_i) + (\xi_i - 2\alpha)\hat{c}_2\hat{c}_5 I_0(a\xi_i)\} + \alpha\{-c_2c_5 I_0(b\xi_0) + c_2c_6 K_0(b\xi_0)\}]\cos\left(\frac{\mathrm{n}\pi\zeta}{\Lambda}\right)$$

$$= C_1 + C_2\zeta + C_3\zeta^2$$

where

$$C_1 = C_{10} + C_{1\omega}$$

$$= \alpha \mathrm{s}^2\left(\hat{\mathrm{c}}_7 + \hat{\alpha}_{11} - 4\hat{\alpha}_6\hat{\alpha}_7{\xi_\mathrm{i}}^2\right) - \alpha \mathrm{s}^2\alpha_7 - \mathrm{L_P}\sigma\Delta\Pi - \mathrm{s}^2\hat{\alpha}_2\hat{\alpha}_4\xi_\mathrm{i} - \mathrm{s}^2\hat{\alpha}_6\hat{\alpha}_7{\xi_\mathrm{i}}^3$$

and

$$C_3 = C_{3\omega} + C_{3cos} = -8\alpha \mathrm{s}^2\hat{\alpha}_6\hat{\alpha}_7$$

$$C_3\zeta^2 = -8\alpha \mathrm{s}^2\hat{\alpha}_6\hat{\alpha}_7\frac{\Lambda^2}{\pi^2}\left(\frac{\pi\zeta}{\Lambda}\right)^2 = -8\alpha \mathrm{s}^2\hat{\alpha}_6\hat{\alpha}_7\frac{\Lambda^2}{\pi^2}\left[\frac{\pi^2}{3} - 4\sum_{n=1}^{\infty}(-1)^{n+1}\frac{\cos\left(\frac{\mathrm{n}\pi\zeta}{\Lambda}\right)}{n^2}\right]$$

$$= -8\alpha \mathrm{s}^2\hat{\alpha}_6\hat{\alpha}_7\frac{\Lambda^2}{3} + 32\alpha \mathrm{s}^2\hat{\alpha}_6\hat{\alpha}_7\frac{\Lambda^2}{\pi^2}\sum_{n=1}^{\infty}(-1)^{n+1}\frac{\cos\left(\frac{\mathrm{n}\pi\zeta}{\Lambda}\right)}{n^2}$$

Because C_1 is constant, $C_2 = 0$, so $C_1 = C_{3\omega}$, and $C_{3\cos}$ = cos term

$$\begin{cases} C_1 + C_{3\omega} = 0 \\ C_{3cos} = \begin{bmatrix} a\{\hat{c}_2\hat{c}_3 I_1(a\xi_i) + (\xi_i - 2\alpha)\hat{c}_2\hat{c}_5 I_0(a\xi_i)\} \\ +\alpha\{-c_2c_5 I_0(b\xi_0) + c_2c_6 K_0(b\xi_0)\} \end{bmatrix}\mathrm{s}^2\cos\left(\frac{\mathrm{n}\pi\zeta}{\Lambda}\right) \end{cases}$$

Comparing it with Fourier Cosine series in equation 3.31

$$[a\{\hat{c}_2\hat{c}_3 I_1(a\xi_i) + (\xi_i - 2\alpha)\hat{c}_2\hat{c}_5 I_0(a\xi_i)\} + \alpha\{-c_2c_5 I_0(b\xi_0) + c_2c_6 K_0(b\xi_0)\}]$$

$$= -16\alpha \frac{(-1)^{n+1}}{n^2} \frac{\omega\Lambda\langle\hat{V}_{zo}\rangle}{{\xi_i}^2\pi^2 s^2} \tag{A-16}$$

BC 12 gives

$$a\xi_i[\hat{c}_2\hat{c}_3 I_1(a\xi_i) + \hat{c}_2\hat{c}_5\xi_i I_0(a\xi_i)]$$

$$- \xi_0[c_2c_3 I_1(\gamma\xi_0) + c_2c_4 K_1(\gamma\xi_0) + c_2c_5 I_1(b\xi_0)$$

$$+ c_2c_6 K_1(b\xi_0)]\}cos\left(\frac{n\pi\zeta}{\Lambda}\right) = -\frac{L_p\Delta\wp{\xi_i}^2}{s^2(2\alpha + \xi_i)}\left(\frac{\zeta}{\Lambda} - \frac{1}{2}\right) \tag{A-17}$$

Comparing it with Fourier Cosine series in equation 3.32

$$\xi_i[\hat{c}_2\hat{c}_3 I_1(a\xi_i) + \hat{c}_2\hat{c}_5\xi_i I_0(a\xi_i)]$$

$$- \xi_0[c_2c_3 I_1(\gamma\xi_0) + c_2c_4 K_1(\gamma\xi_0) + c_2c_5 I_1(b\xi_0) + c_2c_6 K_1(b\xi_0)]$$

$$= \frac{4\Lambda L_p\Delta\wp{\xi_i}^2}{s^2(2\alpha + \xi_i)n^3\pi^3} \tag{A-18}$$

APPENDIX B.

MATLAB PROGRAM USED TO CALCULATE THE CONSTANTS AND GENERATE PLOTS

```
clc
clear all
tic
s=1e6;
r_i=0.00050;
r_o=0.00055;
xi_i=r_i*s;
xi_o=r_o*s;
L=0.02;
lambda=L*s;
mu=0.03;
Lp=21.003e-11;
v_z=1.387;
del_p=28032.00000;
r=0.004;
Z=r*s
a=Lp*s*mu;
b=Lp*del_p/v_z;
w=0.0;
N_sum=100;
N_max=100;

PSITF=zeros(N_max,N_max);
```

```
VZTF=zeros(N_max,N_max);

VRTF=zeros(N_max,N_max);

POUT=zeros(N_max,N_max);

PSICF=zeros(N_max,N_max);

VZCF=zeros(N_max,N_max);

VRCF=zeros(N_max,N_max);

PIN=zeros(N_max,N_max);


%Defining the mesh grid

[xetat,xit]=ndgrid(0:(lambda)/(N_max - 1):lambda,xi_o:(Z-xi_o)/(N_max -

1):Z);%outside

[xetac,xic]=ndgrid(0:(lambda)/(N_max - 1):lambda,0:(xi_i)/(N_max - 1):xi_i);%inside

n=1;

for n=1:N_sum

   m=(n-1)/2;

   an=pi*n/lambda;

   gn=sqrt((an^2)+1);

   a_xi=xi_i*an;

   a_xo=xi_o*an;

   a_Z=Z*an;

   g_xo=gn*xi_o;

   g_Z=Z*gn;
```

```
%matrix
a8i=-Lp*del_p/((2*a+xi_i)*lambda);
a6a7i=-(1/2)*((w*v_z)/(xi_i^2*lambda));
a1a4i=-v_z;
a5a7i=0.5*v_z/((xi_i)^2);
a2a4i=w*v_z/(lambda)-a8i*lambda;
a1a6=w*v_z*xi_i^2/(2*lambda);

K0gZ=besselk(0,g_Z);
I0bZ=besseli(0,a_Z);
K0bZ=besselk(0,a_Z);
b1=0;

K0gxo=besselk(0,g_xo);
I0bxo=besseli(0,a_xo);
K0bxo=besselk(0,a_xo);
b2=0;

I0axi=besseli(0,a_xi);
c2c5in=an*xi_i*besseli(1,a_xi)+2*I0axi;
b3=-((1-(-1)^n)./(2*n.^3))*16*Lp*del_p*lambda/((2*a+xi_i)*pi^3);

I1axi=besseli(1,a_xi);
```

```
I0axi=besseli(0,a_xi);

K1gxo=besselk(1,g_xo);

I1axo=besseli(1,a_xo);

K1axo=besselk(1,a_xo);

b4=-4*(lambda*Lp*del_p*xi_i^2)/((2*a+xi_i)*pi^3)*((1-(-1)^n)./(2*n.^3));


anI1axi=an*besseli(1,a_xi);

c2c5in2=an*besseli(0,a_xi)*(xi_i-2*a);

aK0axo=a*besselk(0,a_xo);

aI0axo=a*besseli(0,a_xo);

b5=-16*a*(-1)^(n+1)*w*lambda*v_z/((2*n-1)^2*xi_i^2*pi^2);


A(1,:)=[0,0,0,I0bZ,K0bZ];

A(2,:)=[0,0,-(gn/an)*K0gxo,I0bxo,-K0bxo];

A(3,:)=[an*I0axi,c2c5in,0,0,0];

   A(4,:)=[an*xi_i*I1axi,an*xi_i^2*I0axi,-xi_o*K1gxo,-xi_o*I1axo,-xi_o*K1axo];

A(5,:)=[anI1axi,c2c5in2,0,-aI0axo,aK0axo];


B=[b1;b2;b3;b4;b5];


C=A\B;

D=A*C;
```

```
c2_c3=C(1,1)

c2_c5=C(2,1)

c2c4=C(3,1)

c2c5=C(4,1)

c2c6=C(5,1)


COST=cos(an*xetat);

SINT=sin(an*xetat);

COSC=cos(an*xetac);

SINC=sin(an*xetac);


    vzt=SINT.*(c2c4*gn*besselk(0,(gn*xit))-
    c2c5*an*besseli(0,(an*xit))+c2c6*an*besselk(0,(an*xit)));


    vrt=COST*an.*(c2c4*besselk(1,(gn*xit))+c2c5*besseli(1,(an*xit))+c2c6*besselk
    (1,(an*xit)));


    vrt2=(1./xit)*(w*xi_i^2/(2*lambda));


    psit=SINT.*(xit.*(c2c4*besselk(1,(gn*xit))+c2c6*besselk(1,(an*xit))+c2c5*bess
    eli(1,(an*xit))));


    presure_t=COST.*(-c2c5*besseli(0,(an*xit))+c2c6*besselk(0,(an*xit)));
```

```
 VZTF=VZTF+vzt;

VRTF=VRTF+vrt;

PSITF=PSITF+psit;

POUT=POUT+presure_t;


VZTFF=VZTF*b;

VRTFF=(VRTF+vrt2)*b;

PSITFF=PSITF*b/(xi_i^2);

PPTFF=a*(POUT-(w*v_z*xi_i^2*log(xit))/(2*lambda));


%inside

    vzc=-
    SINC.*(c2_c5*an*xic.*besseli(1,(an*xic))+(c2_c3*an+2*c2_c5)*besseli(0,(an*x
    ic)));

       vrc=COSC.*(an*(c2_c3*besseli(1,(an*xic))+c2_c5*xic.*besseli(0,(an*xic))));


    psic=SINC.*(c2_c3*xic.*besseli(1,(an*xic))+c2_c5*(xic.^2).*besseli(0,(an*xic)))
    ;


    presure_c=2*a*COSC.*(an*c2_c5*besseli(0,(an*xic)));


VZCF=VZCF+vzc;

VRCF=VRCF+vrc;
```

```
    PSICF=PSICF+psic;
    PIN=(PIN+presure_c);

        vzc1=(-2*a1a4i-4*xic.^2*a5a7i)/v_z;
        vzc2=(-2*xetac.*a2a4i-4*xetac.*xic.^2*a6a7i 2*a8i*xetac.^2)/(Lp*del_p);

        vrc11=(xic*Lp*del_p/(2*a+xi_i)).*(1/2-xetac/lambda);
        vrc22=((xic.*w/lambda)).*(1-0.5*xic.^2/xi_i^2);

        psic1=((xetac.*(xic/xi_i).^2).*(a2a4i+a8i*xetac))./(Lp*del_p);
           psic2=((xic/xi_i).^2).*(a1a4i+xic.^2*a5a7i+a6a7i*xetac.*xic.^2)./(v_z);

        PPCFF=PIN-
        8*v_z*xetac/(xi_i^2)+2*w*(2*xetac.^2+xic.^2)/(xi_i^2*lambda)+4*Lp*del_p.*x
        etac/(lambda*(2*a+xi_i));
end

%[xetac,xic] inside
VRCFF=(VRCF*b+vrc11*b)+vrc22;
VZCFF=((VZCF+vzc2)*b)+vzc1;
PSICFF=(PSICF+psic1)*b+psic2;
```

```
meshc(xetac,xic,PSICFF);%Inside Plotting the velocity

% meshc(xetat,xit,VZTFF);%outside

% Plotting the velocity
```

BIBLIOGRAPHY

Baish, J.W., Netti, P.A., and Jain, R.K. (1997) Transmural Coupling of Fluid Flow in Microcirculatory Network in Tumors. Microvascular Research 53, pp. 128-141.

Baxter, L.T., and Jain, R.K. (1989) Transport of Fluid and Macromolecules in Tumors. I. Role of Interstitial Pressure and Convection. Microvascular Research 37, pp. 77-104.

Baxter, L.T., and Jain, R.K. (1990) Transport of Macromolecules in Tumors. II. Role of Heterogeneous Perfusion and Lymphatics. Microvascular Research 40, pp. 246-263.

Baxter, L.T., and Jain, R.K. (1991) Transport of Macromolecules in Tumors. IV. A Microscopic Model of the Perivascular Distribution. Microvascular Research 41, pp. 252-272.

Baxter, L.T., Zhu, H., Mackensen, D.G., Butler, W.F., and Jain, R.K. (1995) Biodistribution of Monoclonal Antibodies: Scale-up from Mouse to Human using a Physiologically Based Pharmacokinetic Model. Cancer Research 55, pp. 4611-4622.

Boucher, Y., Bracken, C., Netti, P.A., and Jain, R.K. (1998) Intratumoral Infusion of Fluid: Estimation of Hydraulic Conductivity and Implications for the Delivery of Therapeutic Agents. British Journal of Cancer 78, pp. 1442-1448.

Brinkman, H.C. (1947) A calculation of the Viscous Force Exerted by a Flowing Fluid on a Dense Swarm of Particles. Applied Scientific Research Al, pp. 27-34.

Fenster, Aaron, and James C. Lacefield. Ultrasound Imaging and Therapy. CRC Press, Taylor & Francis Group (2015) pp67.

Fournier, R.L. (1999) Basic Transport in Biomedical Engineering, Taylor and Francis, Philadelphia, pp. 44.

Guyton, A.C., and Hall, J.E. (2000) Textbook of Medical Physiology, 10th ed., W.B. Saunders Co., Philadelphia, pp. 163.

Haberman, W.L., and Sayre, R.M. (1958) Motion of Rigid and Fluid Spheres in Stationary and Moving Liquids inside Cylindrical Tubes. U.S. Department of Navy, David Taylor Model Basin Report pp. 1148

Happel, J. (1958) Viscous Flow in Multiparticle Systems: Slow Motion of Fluids Relative to Beds of Spherical Particles. AIChE Journal 4, pp. 197-201.

Jackson, R. (1977) Transport in Porous Catalysts, Elsevier Science Publishing Company, Amsterdam.

Jain, R.K. (1998) Delivery of Molecular and Cellular Medicine to Solid Tumors. Journal of Controlled Release 53, pp. 49-67.

Jain, R.K., and Baxter, L.T. (1988) Mechanism of Heterogeneous Distribution of Monoclonal Antibodies and Other Macromolecules in Tumors: Significance of Elevated Interstitial Pressure. Cancer Research 48, pp. 7022-7032.

Krogh, A. (1991) "The Rate of Diffusion Of Gases Through Animal Tissues, With Some Remarks On The Coefficient Of Invasion."

Mangulis, V. (1965) Handbook of Series for Scientists and Engineers, Academic Press Inc., New York, pp. 90, 95.

Netti, P.A., Roberge, S., Boucher, Y., Baxter, L.E., Jain, R.K. (1996) Effect of Transvascular Fluid Exchange on Pressure-Flow Relationship in Tumors: A Proposed Mechanism for Tumor Blood Flow Heterogeneity. Microvascular Research 52, pp. 27-46.

Saltzman W.M. Drug Delivery: Engineering Principles for Drug Therapy Oxford University Press, Inc., New York (2001)

Schmidt-Schonbein, G. (1999) Biomechanics of Microcirculatory Blood Perfusion. Annual Reviews in Biomedical Engineering 1, pp.73-102.

Sevick, E.M., and Jain, R.K. (1989) Geometric Resistance to Blood Flow in Solid Tumors Perfused Ex Vivo: Effects of Tumor Size and Perfusion Pressure. Cancer Research 49, pp. 3506-3512.

Sevick, E.M., and Jain, R.K. (1991) Measurement of Capillary Filtration Coefficient in a Solid Tumor. Cancer Research 51, pp. 1352-1355.

Tam, C.K.W. (1969) The Drag on a Cloud of Spherical Particles in Low Reynolds Number Flow. Journal of Fluid Mechanics 38, pp. 537-546.

VITA

Xianjie Qiu was born in Guangzhou City, Guangdong Province China. He came to America in Spring 2010 and studied at East Los Angeles College. He transferred to Missouri University of Science and Technology where he earned the Bachelor of Science in Chemical Engineering in December 2015. He received his Master of Science in Chemical Engineering from Missouri University of Science and Technology in July 2018.